RESEARCH PAPER

Identification of TIMING OF CAB EXPRESSION 1 as a temperature-sensitive negative regulator of tuberization in potato

Wayne L. Morris[1,†], Laurence J.M. Ducreux[1], Jennifer Morris[1], Raymond Campbell[1], Muhammad Usman[2], Pete E. Hedley[1], Salomé Prat[3,‡], and Mark A. Taylor[1,*,‡]

[1] The James Hutton Institute, Invergowrie, Dundee DD2 5DA, UK

[2] Institute of Horticultural Sciences, University of Agriculture, Faisalabad 38040, Pakistan

[3] Centro Nacional de Biotecnología, Darwin 3, Campus de Cantoblanco, 28049 Madrid, Spain

[‡] These authors made equal contributions to this work.

[†] In memoriam.

[*] Correspondence: mark.taylor@hutton.ac.uk

Abstract

For many potato cultivars, tuber yield is optimal at average daytime temperatures in the range 14–22 °C. Above this range, tuber yield is reduced for most cultivars. We previously reported that moderately elevated temperature increases steady-state expression of the core circadian clock gene *TIMING OF CAB EXPRESSION 1* (*StTOC1*) in developing tubers, whereas expression of the *StSP6A* tuberization signal is reduced, along with tuber yield. In this study we provide evidence that StTOC1 links environmental signalling with potato tuberization by suppressing StSP6A autoactivation in the stolons. We show that transgenic lines silenced in *StTOC1* expression exhibit enhanced *StSP6A* transcript levels and changes in gene expression in developing tubers that are indicative of an elevated sink strength. Nodal cuttings of *StTOC1* antisense lines displayed increased tuber yields at moderately elevated temperatures, whereas tuber yield and *StSP6A* expression were reduced in *StTOC1* overexpressor lines. Here we identify a number of StTOC1 binding partners and demonstrate that suppression of *StSP6A* expression is independent of StTOC1 complex formation with the potato homolog StPIF3. Down-regulation of *StTOC1* thus provides a strategy to mitigate the effects of elevated temperature on tuber yield.

Keywords: Circadian clock, environment, heat stress, potato, StSP6A, TIMING OF CAB EXPRESSION 1, tuberization.

Introduction

Potato is the leading non-grain commodity in the global food system and the largest tuber food crop in terms of human consumption (Birch *et al.*, 2012). However, a major constraint to tuber yield in potato is its sensitivity to environmental stresses. For example, most commercial potato cultivars are drought sensitive, and potato is particularly vulnerable to increased ambient temperature, which significantly reduces yields (Levy and Veilleux, 2007). Potato is a cool-climate crop, and if the effects of global warming are not mitigated they are predicted to decrease tuber yields by up to 30% by 2050 (reviewed in George *et al.*, 2018).

Elevated temperature impacts on many aspects of potato plant physiology, including inhibition of the tuberization signal

(Ewing, 1981). Recent breakthroughs have elucidated the molecular details of tuberization signalling, leading to a model that explains the inhibition of tuberization in long-day conditions. The central module for photoperiod-sensitive tuberization consists of CONSTANS-like 1 (StCOL1) and an ortholog of FLOWERING LOCUS T (FT) termed StSP6A, which encodes the tuberization signal (Abelenda *et al.*, 2011; Navarro *et al.*, 2011). This mobile 'tuberigen' signal is produced in leaves and moves to the stolon tip, where tuberization is initiated. Expression of this signal is amplified during transport by an autoregulatory mechanism.

Tuberization is repressed in long-day conditions by increased expression of an additional FT homolog (*StSP5G*) acting as a negative regulator of *StSP6A* expression. *StSP5G* is induced in leaves under non-inductive (long-day photoperiod) conditions in a PHYTOCHROME B- and StCOL1- dependent manner (Abelenda *et al.*, 2016). Day-length control of tuberization is linked to the circadian clock components GIGANTEA (StGI) and FLAVIN BINDING KELCH REPEAT F-BOX 1 (StFKF1), which control *StCOL1* expression by signalling degradation of the CYCLING DOF FACTOR 1 (StCDF1) repressors (Kloosterman *et al.*, 2013). Allelic forms of the transcriptional repressors, lacking the C-terminus, were strongly selected during breeding of day-length-insensitive cultivars. Truncation of the C-terminal StFKF1 interaction domain impairs StFKF1–StCDF1 interaction and causes StCDF1 stabilization, which leads to constitutive inhibition of the *StCOL1* gene. Through these studies we have gained good understanding of day-length regulation of the CO-FT module; however, the mechanism by which other environmental cues, such as temperature, affect tuberization are much less clear.

Previously, we observed that increased ambient temperatures suppress *StSP6A* transcript levels, consistent with their inhibitory effects on tuberization (Hancock *et al.*, 2014). Surprisingly, however, expression levels of the *StSP5G* repressor were not elevated in leaves at higher temperature, and were even significantly reduced in tubers. This implies that temperature controls *StSP6A* transcription through other mechanisms than regulation of the *StCOL1–SP5G* expression module. We also investigated the effect of increased temperature on the transcription of core circadian clock genes and observed a rise in the expression levels of *TIMING OF CAB EXPRESSION 1* (*StTOC1*) in developing tubers under warm (30 °C) compared with cooler (22 °C) temperatures over a 24 h period. TOC1 is an evening-expressed protein (Strayer *et al.*, 2000) that is part of a five-member family called the PSEUDO-RESPONSE REGULATORS (PRRs), found in Arabidopsis to be expressed in succession from morning to night in the order *PRR9*, *PRR7*, *PRR5*, *PRR3*, and *TOC1* (Matsushika *et al.*, 2000). PRR proteins consist of two conserved domains, the N-terminal PR (pseudo-receiver) and the C-terminal CCT [CONSTANS (CO), CO-like, TOC1] domain (Wenkel *et al.*, 2006). Interaction between PRRs and other proteins is facilitated by the PR domain (Más *et al.*, 2003; Wang *et al.*, 2011). Purified TOC1 was shown to bind directly to DNA through its CCT domain, although the full range of its downstream targets was not fully elucidated (Gendron *et al.*, 2012).

Evidence for molecular nodes connecting environmental signals with the circadian clock is rapidly emerging (Pokhilko *et al.*, 2013). Intriguingly, Arabidopsis TOC1 has been connected to drought stress responses, via its role in regulating several abscisic acid (ABA) signalling components. *TOC1* expression is induced by ABA in a process that is gated by the clock (Legnaioli *et al.*, 2009). Consistently, plants misexpressing *TOC1* have ABA-dependent stomatal closure defects and altered tolerance to drought stress (Legnaioli *et al.*, 2009). Additionally, Arabidopsis TOC1 was observed to interact with the PHYTOCHROME INTERACTING FACTOR (PIF) family of transcription factors, the C-REPEAT BINDING FACTOR/DEHYDRATION-RESPONSIVE ELEMENT-BINDING (CBF/DREB) proteins, and ABA INSENSITIVE3 (ABI3), respectively involved in hypocotyl elongation, drought and low-temperature responses, and ABA-responsive gene expression (Eriksson and Webb, 2011; Soy *et al.*, 2016).

In view of the altered expression of potato *StTOC1* at elevated temperature and the links between TOC1 and environmental signalling in Arabidopsis, we investigated the potential roles of StTOC1 in linking elevated temperature and potato tuberization.

Materials and methods

Plant material, growth conditions, and phenotyping

Solanum tuberosum L. (cv. Desiree) tissue culture plantlets were propagated in 90 mm petri dishes containing Murashige and Skoog medium (Murashige and Skoog, 1962) supplemented with 20 g l^{-1} sucrose and 8 g l^{-1} agar at 18±4 °C, 16 h light/8 h dark, and light intensity (photosynthetic photon flux density) of 100 μmol m^{-2} s^{-1}. Four weeks after subculture, *in vitro* plantlets were transferred to 12 cm pots containing compost and grown in a glasshouse, under conditions of 16 h light (18 °C) and 8 h dark (15 °C). Light intensity ranged from 400 to 1000 μmol m^{-2} s^{-1} at canopy height. After 8 weeks, plants were transferred to growth cabinets under two different temperature treatments, 22 °C/16 °C or 30° C/20 °C, both with 12 h light/dark, and were watered daily. The light intensity was maintained at 300 μmol m^{-2} s^{-1}. After 2 weeks under controlled conditions, leaves and underground stolons from three replicate plants were harvested. Six to ten swelling stolon tips (3–5 mm in length) were frozen in liquid nitrogen, freeze dried, and stored at –20 °C prior to microarray analysis. For controlled-environment chamber experiments, potato plants were grown from tubers in 30 cm diameter pots at day/night 22 °C/16 °C or 30 °C/22 °C and 12 h night/day cycle, 70% humidity, light intensity of 400 μmol m^{-2} s^{-1} at canopy height, with daily watering. Plants were harvested 80 days post-emergence.

Nodal cutting tuberization assay

Solanum tuberosum L. (cv. Desiree) plants were grown from *in vitro*-propagated tissue culture plantlets in 10 cm diameter pots containing standard compost mix. Plants were raised in a glasshouse maintained at a daytime temperature of 20 °C and a nighttime temperature of 15 °C. Light intensity ranged from 400 to 1000 μmol m^{-2} s^{-1}. Single nodal cuttings consisting of a fully expanded leaf and its subtended bud (Ewing, 1978) were taken from 7–8-week-old plants and the base of the petiole was placed in 50/50 coir/sand mix. Cuttings were kept in glasshouse conditions for 24 h and then moved to growth cabinets set at 70% humidity, 16 h photoperiod, and various temperature regimes (day/night temperatures of 18 °C/14 °C, 24 °C/18 °C, or 26 °C/20 °C). Cuttings were watered daily with prewarmed water. Each treatment was repeated five times with six cuttings per replication. Tubers were harvested after 3 weeks.

Generation of StTOC1 transgenic potato lines

To generate transgenic *StTOC1* antisense and overexpressing potato lines, primers were designed on the PGSC0003DMT400083086 sequence to amplify the 1650 base pair open reading frame from a *S. tuberosum* cv. Desiree tuber cDNA template. *Bam*HI sites were engineered at both termini to facilitate cloning of this fragment. Primer sequences are given in Supplementary Table S3 at *JXB* online. Following *Bam*HI digestion, the fragment was inserted into the *Bam*HI site of pJIT60 and constructs were selected in both the sense and antisense orientations respective to the double 35S promoter. pJIT60 is identical to pJIT30 (Guerineau *et al.*, 1990) but includes a double 35S CaMV promoter. The cloned *StTOC1* fragment was then excised with *Kpn*I and *Xho*I and introduced into the polylinker *Kpn*I and *Sal*I sites of pBIN19.

Microarray methods

A custom Agilent microarray was used, designed to the predicted transcripts from assembly v.3.4 of the DM potato genome as described by Hancock *et al.* (2014). Access to ordering the array design (AMADID 033033) from Agilent is available on request from the authors. The experimental design and complete datasets are available at ArrayExpress (http://www.ebi.ac.uk/arrayexpress/; accession E-MTAB-7443). Briefly, a single-channel microarray design was utilized, with all swelling stolon RNA samples labelled with the Cy3 dye. A total of 16 microarrays were processed, consisting of four biological replicates for the wild-type (WT) and the TOC line for each temperature treatment (22 °C, 30 °C). RNA labelling and subsequent microarray processing was performed as described by Morris *et al.* (2014). Entire feature extraction (Agilent FE v.12.03.02) datasets for each array were loaded as single-channel data into GeneSpring (v.7.3) software for further analysis. Data were normalized using default single-channel settings: intensity values were set to a minimum of 0.01 and data from each array were normalized to the 50th percentile of all measurements on the array. Unreliable data, flagged as absent in all replicate samples by the FE software, were discarded. Statistical filtering of data to identify differentially expressed transcripts between temperature treatments was performed for the control (WT) and transgenic lines independently, using volcano plots. Thresholds of greater than 2-fold change and a Student's *t*-test value of $P \leq 0.01$ were applied. In addition, two-way ANOVA (P-value<0.05) with Benjamini and Hochberg multiple testing correction was used to identify those transcripts showing an interaction between line and temperature. Clustering of gene expression profiles across the time series for the selected ANOVA interaction gene list was performed in GeneSpring using the *K*-means algorithm. Default parameters (100 iterations, Pearson measure as similarity correlation) were used to generate four cluster sets. Gene lists were analysed for gene ontology (GO) term enrichment using the AgriGO v2 package (http://systemsbiology.cau.edu.cn/agriGOv2/; Tian *et al.*, 2017). The Phureja DM1-3 PGSC protein ID for the entire genome was used as background, and Singular Enrichment Analysis was performed using the Fisher test method, Yekutieli false discovery rate, at a P-value≤ 0.05 with a minimum of 10 mapping entries.

RNA extraction and quantitative RT–PCR

RNA was extracted from potato leaves and tubers as described by Ducreux *et al.* (2008). Quantitative reverse transcription (RT)–PCR was performed using an Applied Biosystems StepOnePlus™ system as described by Campbell *et al.* (2010), with primer sequences listed in Supplementary Table S3. Assays were validated by assessing the primer amplification efficiencies as described by Schmittgen and Livak (2008). Primers were designed within the 3′ untranslated region to assess the level of down-regulation of endogenous *StTOC1* expression. The reactions were repeated in triplicate with independent cDNAs and relative expression levels were calculated as described previously (Schmittgen and Livak, 2008). For normalizations, expression of *ef1α* was used, as expression of this gene in potato is stable over a wide range of abiotic and biotic stresses (Nicot *et al.*, 2005).

Yeast two-hybrid screening of a potato cDNA library

To identify StTOC1 interaction partners, a yeast two-hybrid potato leaf library (Bos *et al.*, 2010) was screened, using StTOC1 as the bait, using the ProQuest™ Two-hybrid system (Invitrogen). *StTOC1* was transferred from the pDONR201 entry vector (described above) into the destination vector pDEST™32 by LR recombination using Gateway® technology according to manufacturer's instructions (Invitrogen). The resulting pEXP™32-TOC1 construct was transformed into the yeast strain MaV203, and transformants were recovered by SD-Leu nutritional selection. A single colony was grown and used to prepare competent yeast cells that were subsequently transformed with a commercially prepared potato yeast two-hybrid library (Bos *et al.*, 2010). Transformants were plated on SD –LTH/ SD –LTU growth media for selection of interacting candidates. Plasmids were isolated from the positive colonies and co-transformed into MaV203 with either pEXP™32-TOC1 or the empty bait vector pDEST™22 to eliminate false positives. Translated nucleotide sequences of positive clones were searched (BLASTP) against the Spud DB transcripts database (v3.4) to retrieve the ITAG annotations, and were subsequently used to identify the Arabidopsis homologues (TAIR10 proteins database). A reciprocal BLASTP of Spud DB (ITAG) using TAIR protein sequence was performed to verify hit identities.

Co-immunoprecipitation and bimolecular fluorescence complementation studies

The *StPIF3* and *StTOC1* open reading frames (ORFs) were amplified from a cDNA prepared from *S. tuberosum* cv. Desiree, by using primers containing the Gateway® recombination (attB) sites, and cloned into pDONR201 according to the manufacturer's instructions (Invitrogen). The *StPIF3* and *StTOC1* ORFs were then transferred to the binary vectors pGWB6 and pGWB15 to create N-terminal tagged green fluorescent protein (GFP) and haemagglutinin (HA) constructs, respectively. Transgenic lines containing the StTOC1-HA fusion construct were generated using the transformation protocol described above. For co-immunoprecipitation studies, constructs were transformed into *Agrobacterium tumefaciens* strain GV3101. Bacterial cultures expressing these plasmids were used for infiltration of *Nicotiana benthamiana* leaves, together with the p19 protein to suppress gene silencing. To that end, single colonies were grown at 28 °C overnight in 10 ml YEB medium with kanamycin at 50 mg l^{-1} and rifampicin at 10 mg l^{-1}; bacterial pellets were resuspended in 5 ml 10 mM MES, pH5.8, 10 mM MgSO4, 150 μM acetosyringone, and incubated for 2 h with shaking at room temperature. *Agrobacterium* cells expressing the tagged protein constructs were diluted to OD$_{600}$=0.7 and those bearing the p19 plasmid to OD$_{600}$=1.0, and 1:1:2 volumes of these cell suspensions in MES–MgSO4 buffer were used for infiltration. The next day, leaves were treated with 10 μM MG132, and 24 h later they were frozen in liquid nitrogen. For immunoprecipitation, 250–500 mg of the powdered leaf material was homogenized in 2 volumes extraction buffer (50 mM Tris–HCl, pH 7.5, 10 mM MgCl$_2$, 150 mM NaCl, 2.5 mM EDTA, 10% glycerol, 25 mM β-glycerophosphate, 0.1% NP-40, 10 mM NaF, 2 mM Na$_3$VO$_4$, 100 μM PMSF, 5 μM β-mercaptoethanol, and protease inhibitors), cleared by two rounds of centrifugation at 18 400 *g* for 5 min at 4 °C, and incubated for 4 h with 40 μl anti-HA agarose beads (Sigma). Beads were collected by a brief spin-down at 6000 *g*, washed five times with 500 μl extraction buffer, and eluted by boiling in 50 μl SDS-loading buffer for 3 min. Volumes of 10 μl and 40 μl of the eluted fraction were separated on SDS-PAGE gels to allow immunoblot detection of the immunoprecipitated HA-StTOC1 and pulled-down GFP-StPIF3 or GFP-StSP6A proteins with anti-HA-HRP (Roche) and anti-GFP-HRP (Milteny) antibodies. Leaves expressing the GFP-StPIF3 or GFP-StSP6A proteins alone were used as a control for non-specific binding to the beads. Proteins in the different fractions were visualized with the Supersignal West Pico and Femto substrates (Pierce).

For bimolecular fluorescence complementation (BiFC) studies, the full-length StPIF3, StTOC1, and StSP6A proteins were directly inserted after the N- and C-terminal fragments of yellow fluorescent protein (YFP), by LR clonase incubation of the respective pDONR201 and

pENTRY S/D TOPO clones with the binary YFN43 and YFC43 BiFC vectors (Belda-Palazón *et al.*, 2012). The resultant plasmids were transformed into the *A. tumefaciens* strain GV3101, and *N. benthamiana* leaves were infiltrated with the different strain combinations expressing the YFP^N and YFP^C protein fusions or the empty vectors, along with the p19 silencing suppressor. Bacterial cultures were suspended in MES–MgSO4-acetosyringone solution as for the co-immunoprecipitation studies. Two days after infiltration, leaves were observed under a Leica TCS SP8 laser scanning confocal microscope, using an Excitation Beam Splitter TD 488/561/633 and emission band width between 495 and 556 nm.

Transient transactivation assay studies

For transactivation studies, the *p6A*_for: 5′-CACCTGTTAATTTCCTT TCTT-3′ and *p6A*_rev: 5′-CTCTAGGCTTGATAAAATTAAGT-3′ primers were designed to amplify the 2.64 kb upstream start codon region of the PGSC0003DMT400060057 sequence. The PCR product was cloned into pENTRY S/D TOPO and mobilized by LR clonase recombination into the pLuc-Trap3 vector, to generate the *p6A*::LUC construct. For luciferase assays, *N. benthamiana* leaves were co-infiltrated with *Agrobacterium* strains expressing this reporter and the *35S*::GFP-StPIF3, *35S*::HA-TOC1, and *35S*::GFP-SP6A effector constructs, in the indicated combinations, along with the p19 silencing suppressor. Bacterial cultures expressing the *p6A*::LUC reporter were used at OD_{600}=0.3, and the effector and p19 strains at OD_{600}=0.7 and 1.0, respectively. To test the activity of the reporter alone, or LUC activity levels driven by just one of the effectors, bacterial cultures were mixed with an *Agrobacterium* strain expressing the empty pGWB6 vector, to prevent differences in LUC expression due to dilution effects. Two days after infiltration, leaf discs of 0.6 cm diameter were collected from the leaves and transferred to 96-well microtitre plates containing 195 μl 0.5× Murashige and Skoog liquid medium and the D-luciferin (Promega) substrate (5 μg ml^{-1}). Luminescence was measured with a LB 960 Microplate Luminometer (Berthold). One disc was used per well and at least 12 disc replicates were measured per sample. The median of the activity values and standard error were represented.

Results

StTOC1 *misexpression affects tuberization signalling at elevated temperature*

We have previously shown that *StTOC1* expression is constitutively elevated in developing tubers under moderately elevated temperature (Hancock *et al.*, 2014). To test whether this elevated expression had an impact on tuber yield, we generated transgenic lines down-regulated in *StTOC1* expression in the *S. tuberosum* cultivar Desiree. Leaves from 27 independent tissue-cultured transgenic lines expressing the *StTOC1* gene in antisense orientation were screened by quantitative RT–PCR to assess the inhibition of the endogenous gene (Fig. 1A). For all lines tested there was a significant decrease in endogenous *StTOC1* expression. Three lines (TOCAS32, TOCAS44, and TOCAS67) displaying the strongest silencing were selected for further analysis and grown to maturity to assess *StTOC1* transcript levels in tubers, which ranged from 50% to 20% of those in the WT (Fig. 1B). A statistically significant 19–31% increase in plant height was observed in these transgenic lines compared with WT controls (Supplementary Fig. S1), consistent with the reported phenotype of Arabidopsis *toc1-1* mutants (Más *et al.*, 2003). For more detailed gene expression analysis, a line exhibiting strong *StTOC1* transcript reduction was selected (TOCAS44). Tubers derived from the primary TOCAS44 line were propagated and swelling stolons
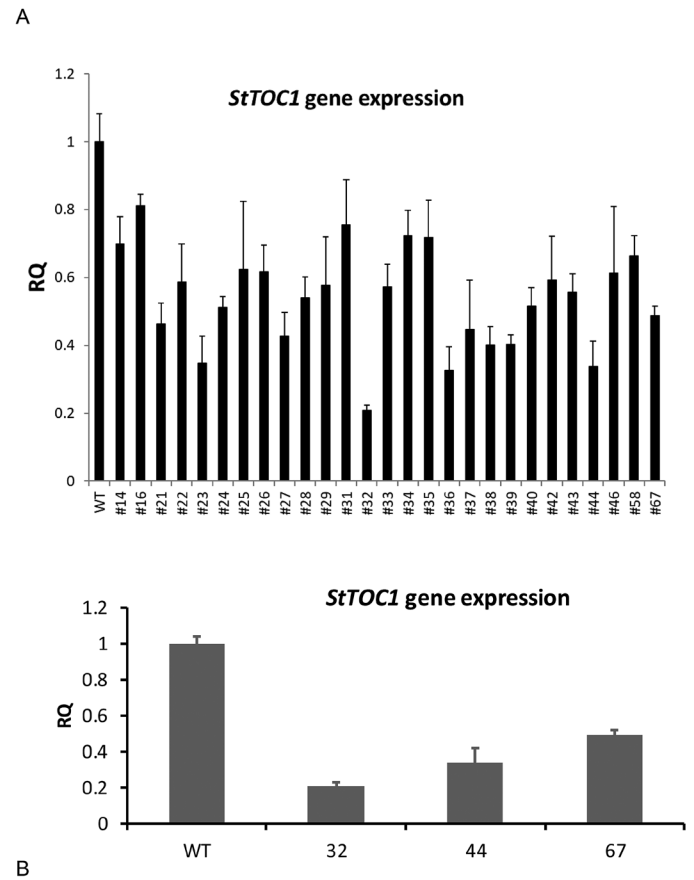

Fig. 1. (A) Quantitative RT–PCR of primary transgenic tissue culture leaves to assess the level of *StTOC1* expression. RQ, relative quantitation. Error bars represent the SE of three biological replicates. *StTOC1* expression was significantly lower than in wild-type (WT) controls as determined by Student's *t*-test (P<0.05). (B) Gene expression analysis as determined by quantitative RT–PCR for tubers of selected Desiree *StTOC1* antisense transgenic lines (TOCAS32, TOCAS44, and TOCAS67) compared with the WT control. Error bars represent the SE of three biological replicates. *StTOC1* expression was significantly lower than in WT controls as determined by Student's *t*-test (P<0.05).

were harvested from independent replicates for gene expression analysis at 22 °C and 30 °C. Expression of the *StTOC1* gene was down-regulated in these plants at both temperatures (Fig. 2). Comparison of *StSP6A* transcript levels between the WT and the TOCAS44 line revealed a significant increase (264%, *P*=0.036) at 30 °C, suggesting that lower expression of *StTOC1* suppresses the negative effects of temperature on expression of the tuberization signal (Fig. 2). As observed previously (Hancock *et al.*, 2014), *StSP5G* transcript levels were reduced in swelling stolons at elevated temperature, and a trend towards a smaller degree of inhibition was observed in TOCAS44 lines. This effect was stronger at 22 °C, while differences at 30 °C were not statistically significant compared with the WT (Fig. 2C).

Enhanced tuber yield of TOCAS lines in a nodal cutting tuberization system

To determine whether the enhanced *StSP6A* transcript level in *StTOC1*-silenced lines correlated with increased tuber
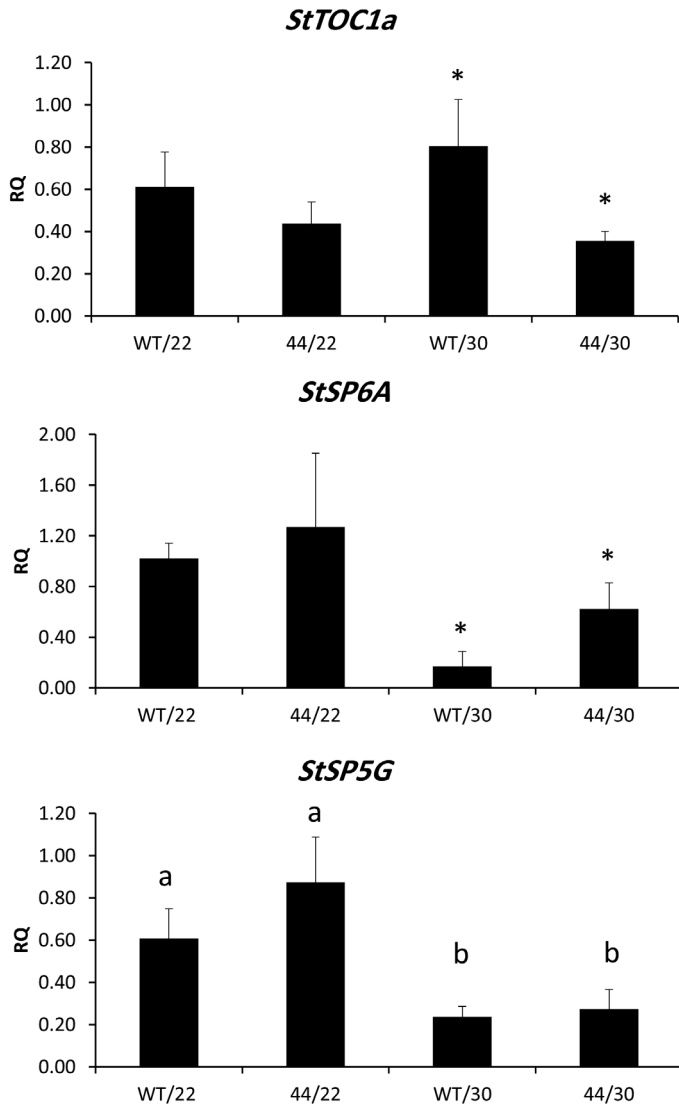
StTOC1a

StSP6A

StSP5G

Fig. 2. Gene expression levels of *StTOC1*, *StSP6A*, and *StSP5G* as determined by quantitative RT–PCR of swelling stolons from line TOCAS44 compared with the wild type (WT) control. Plants were grown at normal (22 °C) and elevated (30 °C) temperature. RQ, relative quantitation. Error bars represent the SE of three biological replicates. Significant differences in expression in the transgenic lines as estimated using Student's *t*-test are indicated by asterisks (*P*<0.05). Values labelled with the same letter were not significantly different based on one-way ANOVA with Fisher's least significant difference test.

yield, we employed a nodal cutting tuberization system, first described by Ewing and Wareing (1978) and utilized more recently in a genetic screen for heat tolerance in potato (Trapero-Mozos *et al.*, 2018). Incubation of the nodal cuttings in controlled-environment chambers enabled tuberization to be monitored at different temperatures.

In WT Desiree, there was a decrease in the fresh weight of tubers (58%) as the temperature increased from night/day 14 °C/18 °C to 20 °C/26 °C. In contrast, tuber yield improved in TOCAS lines at the elevated temperature (Fig. 3) and reached up to 147% of the yield under lower-temperature conditions. This enhancing effect of temperature on tuber yield contrasted with the reduced tuber yield in WT cuttings and was consistently reproduced in subsequent experiments.
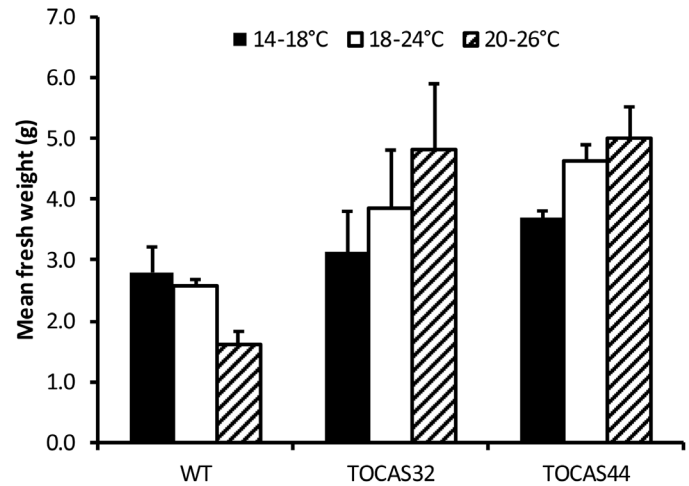

Fig. 3. Comparison of tuber yields at normal (18 °C) and elevated (24, 26 °C) temperature from nodal cuttings of TOCAS32 and TOCAS44 lines compared with the wild type (WT) control. Error bars represent the SE of difference from ANOVA of the interaction term (line and temperature).

A two-way ANOVA, considering the factors line (or genotype) and temperature, showed that the difference in yield was significant. Using a multiple comparison test (Fisher's protected least significant difference) the WT was significantly different to all antisense lines. The interaction term (line and temperature) was also significant (*P*=0.018), showing that TOCAS lines respond differently to temperature.

In order to validate the results obtained from the nodal cutting tuberization system, a yield experiment was conducted using pot-grown plants, comparing the tuber yield of the WT Desiree and TOCAS44 lines grown in a controlled-environment chamber. For plants grown under night/day 16 °C/22 °C temperatures, there was no significant difference in tuber yield, dry matter content, or tuber number (Supplementary Fig. S2A). In contrast, tuber yield was reduced for plants grown under night/day 22 °C/30 °C temperatures, but this effect was significantly less pronounced (~40%) for TOCAS44 lines than for the WT. Tuber number was also elevated under higher-temperature conditions (by ~41%), although this response was similar in the WT and TOCAS44 lines (Supplementary Fig. S2B). Thus, the higher yield at elevated temperature for TOCAS44 plants was due to higher tuber weight (~50%) compared with the WT (Supplementary Fig. S2C).

Constitutive overexpression of StTOC1 results in reduced StSP6A expression and tuber yield

Sets of transgenic lines were generated in which *StTOC1* was overexpressed under control of the constitutive *35S* CaMV promoter. Tuber yield was determined using the nodal cutting assay (Fig. 4A) and, contrary to the effects of decreased *StTOC1* levels, overexpression of StTOC1 resulted in decreased tuber yield in all three independent lines tested (by ~50% compared with controls). Using a two-way ANOVA, considering the effects of genotype and temperature, there was a significant difference between the WT and transgenic lines. A multiple comparison test (Fisher's protected least significant difference) likewise showed that tuber yield was significantly
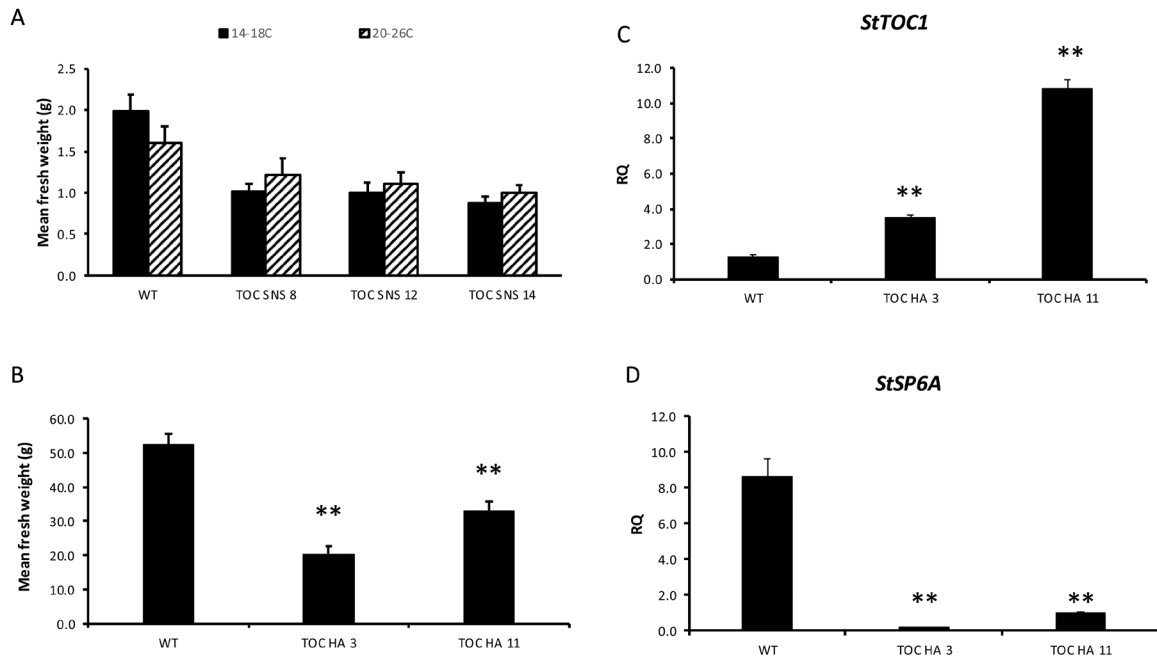
Fig. 4. (A) Comparison of tuber yields at normal (14–18 °C) and elevated (20–26 °C) temperature from nodal cuttings of Desiree *StTOC1* sense lines TOCSNS8, TOCSNS12, and TOCSNS14 compared with the wild type (WT). Error bars represent the SE of difference from ANOVA of the interaction term (line and temperature). (B) Comparison of tuber yield in stem node cuttings from WT plants and lines TOCHA3 and TOCHA11 overexpressing the tagged StTOC1-HA protein. Plants were grown at a daytime maximum temperature of 18 °C. Significant differences between transgenic lines and the WT, as estimated using Student's *t*-test, are indicated by asterisks ($P<0.01$). (C, D) Comparison of gene expression levels of *StTOC1* (C) and *StSP6A* (D) as determined by quantitative RT–PCR of leaves from lines TOCHA3 and TOCHA11 compared with WT. Plants were grown at a daytime maximum temperature of 18 °C. RQ, relative quantitation. Error bars represent the SE of three biological replicates. Significant differences between transgenic lines, as estimated using Student's *t*-test, are indicated by asterisks ($P<0.01$).

different in the WT compared with all overexpressing lines. Transgenic lines overexpressing *StTOC1* tagged with the HA epitope at the C–terminus were also generated. As for *StTOC1* overexpressers, a significant decrease in tuber yield was observed in nodal cuttings of the tagged lines grown at a daytime maximum temperature of 18 °C (Fig. 4B). Gene expression analyses showed that *StTOC1* transcript levels were strongly up-regulated in leaves (by 11-fold for line TOCHA11) in both transgenic lines tested (Fig. 4C), and this was correlated with a significant decrease (~8-fold) in the expression level of *StSP6A* (Fig. 4D). Moreover, in contrast to the silenced lines, *StTOC1* overexpressers displayed a statistically significant decrease in plant height compared with WT controls (Supplementary Fig. S1), indicative of a conserved function of potato StTOC1 in the circadian control of plant growth.

StTOC1 *screening of a yeast two-hybrid library*

Previously, several studies have identified proteins that interact with Arabidopsis TOC1 (Eriksson and Webb, 2011; Soy *et al.*, 2016). Interaction with these partners modifies TOC1 function and has a relevant role in linking light signals to both circadian and photomorphogenic processes. To identify StTOC1 partners with a role in tuberization, a yeast two-hybrid potato leaf library (Bos *et al.*, 2010) was screened using StTOC1 as the bait. This screen identified 10 StTOC1-interacting proteins, including StPIF3 (Table 1; Supplementary Fig. S3). Complex formation with this PIF potato homolog was confirmed by co-immunoprecipitation (Supplementary Fig. S3). TOC1 is

shown in Arabidopsis to repress the transcriptional activity of PIFs (Soy *et al.*, 2016), and this interaction was studied in more detail in transactivation assays.

Transactivation assays of SP6A using the TOC1 OX construct

To determine whether the StTOC1 protein plays a role in *StSP6A* regulation, transient transactivation assays were performed. The *StSP6A* promoter (2.64 kb) was fused to the luciferase reporter gene (*p6A*::LUC), and this reporter construct was agroinfiltrated into *N. benthamiana* leaves alone or in combination with constructs expressing the StTOC1 and/or StSP6A effector proteins. Since we showed StPIF3 to be a StTOC1-interacting partner (Supplementary Fig. S3), we also tested whether complex formation with this PIF factor is involved in *StSP6A* promoter regulation (Fig. 5). Notably, StTOC1 was observed in these assays to suppress *StSP6A* promoter activity, and this inhibition was much greater when *StTOC1* was co-infiltrated with the StSP6A protein than when expressed alone. Although previous studies have demonstrated that StSP6A activates its own expression in stolons (Navarro *et al.*, 2011), a marginal activation of the *p6A*::LUC reporter was observed on expression of the StSP6A effector alone. This implies that an additional DNA-binding protein not present in *N. benthamiana* leaves is required for this regulation. The finding that StTOC1 suppresses expression of the *p6A*::LUC reporter, however, is fully consistent with the expression data of swelling stolons, where *StSP6A* transcript levels were increased

Table 1. *List of proteins shown to interact with StTOC1 by screening of a potato yeast two-hybrid cDNA library*

| Top SpudDB hit (ITAG annotation)	SpudDB identifier	Top Arabidopsis hit (TAIR annotation)	TAIR identifier
Helix-loop-helix DNA-binding	Sotub01g039200.1.1	StPIF3, Phytochrome interacting protein3	At1g09530
Pentatricopeptide repeat-containing protein	Sotub11g006500.1.1	SVR7, Suppressor of variegation7	At4g16390
Retinoblastoma-binding protein	Sotub10g025990.1.1	DWNN domain, a CCHC-type zinc finger	At5g47430
Nucleotidyltransferase	Sotub01g033170.1.1	Nucleotidyltransferase	At3g61690
Mahogunin	Sotub01g036450.1.1	RING/U-box superfamily protein	At3g06140
SAT5, cell number regulator 8-like	Sotub09g007070.1.1	PLAC8 family protein	At2g37110
Pseudo-response regulator5	Sotub03g016990.1.1	Pseudo-response regulator5	At5g24470
ATP binding protein	Sotub02g022320.1.1	Octicosapeptide/Phox/Bem1p family protein	At4g05150
DNA binding protein	Sotub01g048540.1.1	Basic Helix-Loop-Helix 121	At3g19860
Class II chitinase	Sotub02g026280.1.1	Basic Chitinase	At3g12500
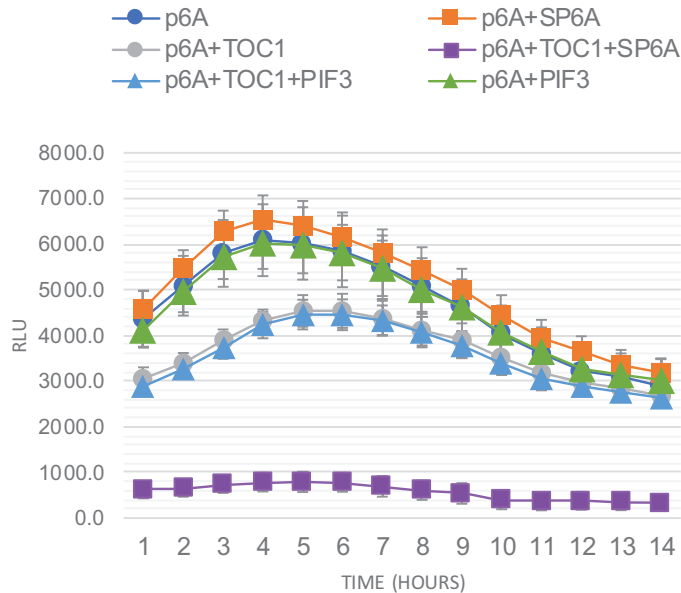
Fig. 5. Relative luminescence units (RLU) from transient expression studies of the 2.64 kb *StSP6A* promoter fused to the LUC reporter gene (*p6A*::LUC) co-transformed with the *35S*::StTOC1, *35S*::StPIF3, and *35S*::StSP6A effector constructs. *Agrobacterium tumefaciens* cells containing these constructs were co-infiltrated into *N. benthamiana* leaves and luciferase activity was measured in excised leaf discs at intervals of 1 h for 14 h. Error bars represent the SD of *n*=12 leaf discs. Studies were repeated three times, with similar results.

in the *StTOC1* down-regulated lines (Fig. 2). This observation reflects that StTOC1 acts as an inhibitor of the *StSP6A* autoregulatory loop, possibly by interfering with the transcriptional activity of StPIF3 (Soy *et al.*, 2016). However, StPIF3 did not induce *p6A::LUC* activity when expressed either alone or in combination with StTOC1 (Fig. 5), which suggests that StTOC1–StPIF3 complex formation may have a relevant role in the growth effects observed upon *StTOC1* misexpression, but it is not directly involved in the regulation of *StSP6A*.

StTOC1 interactions in planta

GFP-tagged proteins for StPIF3, StTOC1, and StSP6A were localized following infiltration of *N. benthamiana* leaves (Supplementary Fig. S4). Remarkably, the GFP-StPIF3 and GFP-StTOC1 proteins localized to nuclear bodies, whereas StSP6A-GFP was distributed in both the cytoplasm and

nucleus, as previously observed for other PEBP proteins (Zhan *et al.*, 2017).

We further analysed StTOC1 *in planta* interactions by using BiFC assays, where the N- or C-terminal portions of YFP were fused to StTOC1, StPIF3, and StSP6A. *Agrobacterium* strains expressing these fusions were infiltrated into *N. benthamiana* leaves, and reconstituted fluorescence by these proteins was assessed using confocal microscopy (Fig. 6). Interaction in the nucleus was observed between StTOC1 and StSP6A (Fig. 6A), StTOC1 and StPIF3 (Fig. 6E) and StTOC1 with itself (Fig. 6D). No interaction was evident between StSP6A and StPIF3 (Fig. 6B); negative controls are shown in Fig. 6C, F. Very low levels of fluorescence were observed in leaves expressing the YFP[N]-StSP6A protein and the empty YFC43 vector (Fig. 6C), used as a negative control. However, this signal was much weaker than for the YFP[N]-SP6A and YFP[C]-TOC1 proteins, and, similarly to the GFP-SP6A tagged protein, it was distributed in both the nucleus and cytosol. In addition, yellow fluorescence as a result of YFP[C]-StTOC1 and YFP[N]-StPIF3 interaction initially had a diffuse pattern but formed nuclear speckles following light irradiation (evident in Fig. 6I), as expected for a phytochrome–interacting factor (Possart *et al.*, 2017). Therefore, BiFC confirmed an *in vivo* interaction of the StSP6A and StTOC1 proteins in the nucleus (Fig. 6A), as implied by the transactivation experiments (Fig. 5). Co-immunoprecipitation studies further corroborated the interaction between StSP6A and TOC1 (Supplementary Fig. S3), thus unveiling a major role of this complex in the negative control of the *StSP6A* autoregulatory loop.

Changes in gene expression in swelling stolons associated with StTOC1 down-regulation

Transcriptomic analyses were performed using a custom Agilent microarray (see Materials and methods) containing probes representing transcripts of all 39 031 protein–coding genes predicted from the potato genome sequence (The Potato Genome Consortium, 2011).

For the identification of genes that differentially respond to elevated ambient temperature in the transgenic lines, transcripts whose expression levels displayed a significant interaction with respect to genotype and temperature (594 probes) were identified by two–way ANOVA. A GO enrichment analysis using the AgriGO v2 platform (Tian *et al.*,
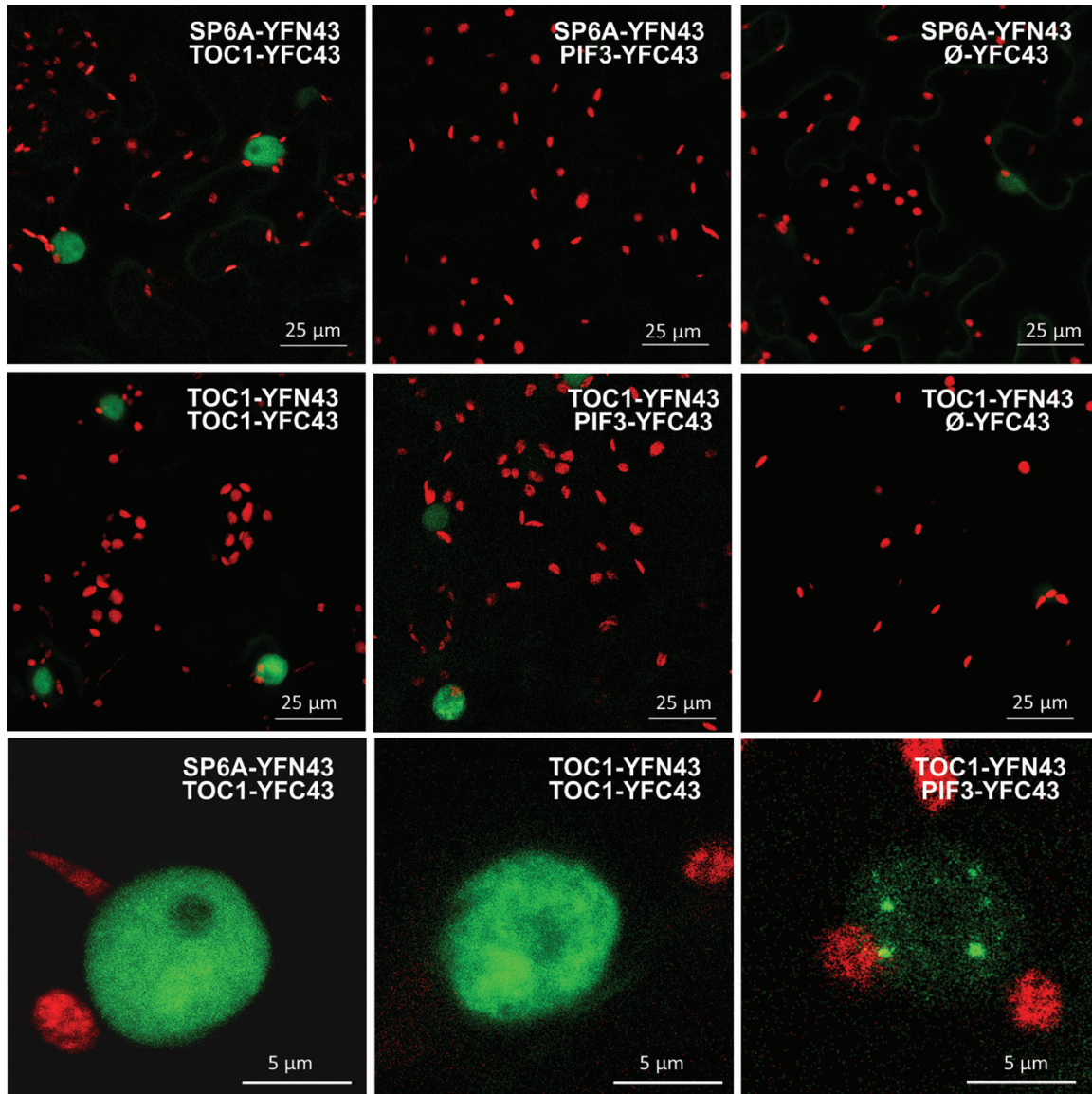
Fig. 6. *In planta* protein–protein interactions between StTOC1, StPIF3, and StSP6A. Representative confocal microscopy images showing the reconstituted BiFC fluorescence in epidermal *N. benthamiana* cells. YFP fluorescence generated by protein–protein interaction was detected 2 days after infiltration. The interactions tested are indicated in panels A–I. (C) and (F) show the StSP6A-YFN43 and StTOC1-YFN43 fusions infiltrated with the empty YFC43 vector, used as negative controls. Weak fluorescence in the cytosol and nucleus was observed for the StSP6A-YFN43 negative control (C). Strong fluorescence by the reconstituted YFP protein (A) denotes that StSP6A and StTOC1 interact in the nucleus. BiFC studies confirmed a nuclear interaction of the StPIF3 and StTOC1 proteins (E), and the dimerization of StTOC1 (D). No YFP fluorescence was observed in leaves infiltrated with the StSP6A-YFN43 and StPIF3-YFC43 constructs (B), indicating that these proteins do not interact. (G), (H), and (I) are higher magnifications of (A), (D), and (E), respectively.

2017) showed that these 594 probes were enriched in several terms related to cellular and metabolic processes (Fig. 7). Further cluster analysis, using the *K*-means clustering algorithm, grouped this gene set into four main clusters (Supplementary Fig. S5), listed in Supplementary Table S2. This table also includes the GO annotation for each probe in the list. Cluster 4 groups 64 genes with particularly marked up-regulation in TOCAS swelling stolons (Supplementary Table S2). This dataset includes the multicystatin, beta-expansin 1, chitin-binding lectin, and polyphenol oxidase genes, which showed 39-fold, 11-fold, 9-fold, and 9-fold increases, respectively, in the TOCAS44 line at 30 °C compared with the WT at 22 °C.

We further examined the expression patterns of sets of genes that have been previously identified as having important roles in tuber development. For example, genes related to starch biosynthesis have been defined in previous studies (Ferreira *et al.*, 2010; Van Harsselaar *et al.*, 2017), and displayed at time point ZT0 striking differences in expression levels between the WT and TOCAS44 tuberizing stolons, under both normal and elevated temperatures (Supplementary Table S1). Most genes involved in starch metabolism were expressed at lower levels at 22 °C in the WT compared with TOCAS44, suggesting that *StTOC1* affects starch synthesis at normal temperatures. In addition, comparison of the expression levels of starch-related genes at elevated temperature revealed a general trend towards
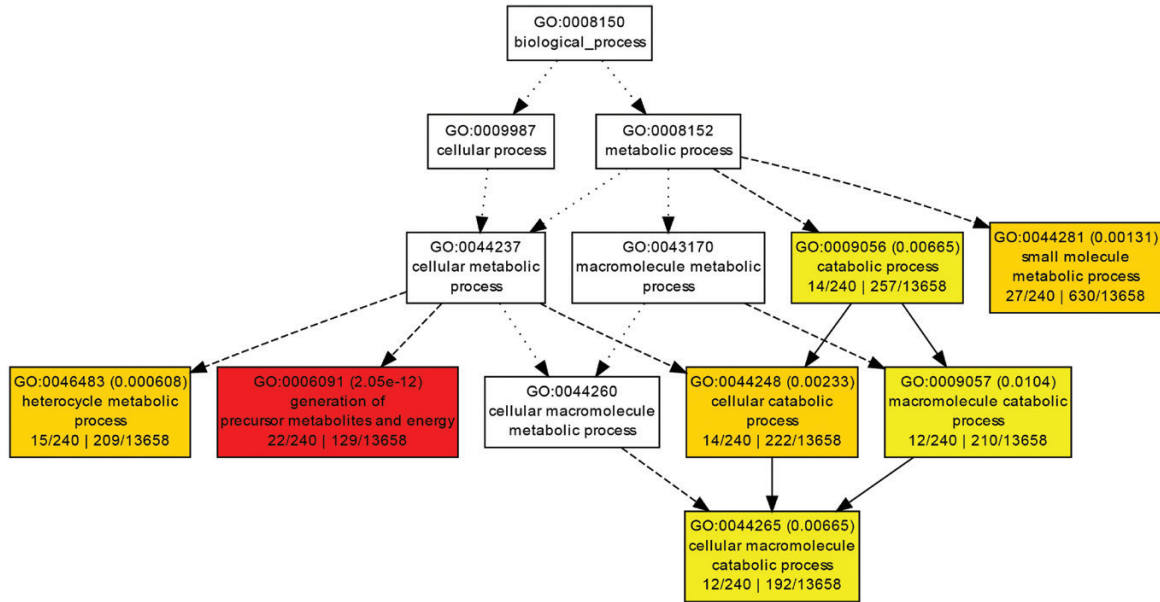
Fig. 7. Hierarchical tree graph showing the over-represented AgriGO v2 GO terms for the genes differentially expressed in TOCAS swelling stolons, The Phureja DM1-3 PGSC protein ID for the entire genome was used as background, and the expression data were analysed using the Fisher test method, Yekutieli false discovery rate, at a P-value≤0.05, with a minimum of 10 mapping entries. Boxes represent GO terms labelled by their GO ID. Box colours indicate significance (e) levels: lower e-values are red, through orange, to yellow for higher e-values; non-significant terms are shown in white boxes.

higher expression in the TOCAS44 line. As StTOC1 suppresses the impact of heat by enhancing tuber yield, we also analysed the abundance of heat shock response transcripts in these samples. Genes encoding heat shock proteins were expressed at a higher level in the TOCAS44 stolons compared with the WT at 22 °C. The increase in expression of heat shock proteins at elevated temperature was also stronger in the TOCAS44 lines than in the WT (Supplementary Table S1).

Discussion

Environmental control of tuberization

The molecular basis of the photoperiodic control of tuberization is firmly established and key regulatory modules have been described (Abelenda *et al.*, 2011; Navarro *et al.*, 2011; Kloosterman *et al.*, 2013; Abelenda *et al.*, 2016). In view of the sensitivity of tuberization to moderately elevated temperature, we studied whether the same regulatory modules integrate temperature cues or, rather, involve additional temperature-responsive mechanisms. It has previously been demonstrated that elevated temperature affects tuber development by inhibiting the expression of the tuberization signal (Ewing, 1981; Hancock *et al.*, 2014). However, elevated temperature is known to affect multiple processes in potato plant physiology. For example, carbon transport to sink organs and the incorporation of assimilated carbon into starch in the tuber are both reduced at elevated temperatures (Wolf *et al.*, 1991). Photosynthetic performance is adversely affected alongside tuber formation, as heat leads to chlorophyll loss and reduced CO_2 fixation (Reynolds *et al.*, 1990).

Clues as to how the circadian clock is linked to temperature inhibition of the tuberization signal were obtained from expression studies, which demonstrated that *StTOC1*

expression increased at elevated temperature in developing tubers (Hancock *et al.*, 2014), leading us to investigate the effects of *StTOC1* misexpression in transgenic lines.

Phenotypic effects of altered StTOC1 expression

Gene expression patterns were compared in *StTOC1* antisense lines and WT controls under standard and moderately elevated temperature conditions. At 30 °C, down-regulation of *StTOC1* expression was associated with increased *StSP6A* transcript levels in swelling stolons, suggesting that under these conditions *StTOC1* is a negative regulator of tuberization (Fig. 2). Consistent with these data, the tuber yields of *StTOC1* antisense lines nodal cuttings were higher at moderately elevated temperature than in the controls (Fig. 3). We have recently demonstrated that the nodal cutting system can be used to predict the tuber yield performance of whole plants under elevated temperature (Trapero-Mozos *et al.*, 2018). In the current work, the effect of enhanced tuber yield at elevated temperature in *StTOC1* antisense lines was also observed in a whole-plant experiment, where higher tuber yields were observed to be due to an increase in mean tuber size (Supplementary Fig. S2). Additional work will be required to determine whether this effect is due to earlier tuberization or an accelerated rate of tuber bulking. To further support a negative effect of StTOC1 on tuberization, we also generated transgenic lines in which *StTOC1* was overexpressed. In contrast to the antisense lines, in these lines tuber yield was reduced, and overexpression of *StTOC1* was seen to reduce *StSP6A* expression in leaves (Fig. 4).

In addition to its effects on tuberization, the *StTOC1* expression level also impacted on plant height, as antisense lines showed an elongated above-ground phenotype compared with the WT, whereas overexpressing lines showed a decrease in plant height (Supplementary Fig. S1). Previously, similar effects on

hypocotyl elongation have been reported for Arabidopsis TOC1, due to an interaction of TOC1 and PIFs inhibiting the transcriptional activity of these factors (Más *et al.*, 2003, Soy *et al.*, 2016). *StSP5G* was observed to be increased in tubers from *StTOC1* down-regulated lines, in contrast to expectations for a primary negative regulatory role of StSP5G on *StSP6A* expression in the tuber (Fig. 2). Previous studies using grafting experiments indicate that StSP5G has a major repressive action on *StSP6A* expression in leaves, but this negative control is less important in below-ground tissues (Navarro *et al.*, 2011). This tissue-specific regulation is consistent with the expression patterns we previously observed in developing tubers from potato plants undergoing moderate heat stress (Hancock *et al.*, 2014). Global gene expression profiling analyses of swelling *StTOC1* antisense stolons, using the Agilent 60-mer microarray platform, showed that genes related to starch metabolism were strongly up-regulated under normal and moderately elevated temperatures in the transgenic lines, which supports the notion that StTOC1 is a negative regulator of tuberization (Supplementary Table S1). Analysis of genes encoding heat shock proteins also revealed a greater capacity of the transgenic lines to respond to an increase in temperature compared with the WT controls.

Many genes previously identified as being stress responsive were also elevated in *StTOC1* down-regulated lines, including those encoding multicystatin, polyphenol oxidase, chitin-binding lectin, and beta expansin 1. Phytocystatin and polyphenol oxidases have been reported to be activated in response to abiotic stress (Halford and Foyer, 2015). Likewise, overexpression of a wheat expansin gene in tobacco was described to confer enhanced tolerance to oxidative stress (Han *et al.*, 2015). These observations, coupled with other reports implicating StTOC1 in additional stress responses, make these transgenic lines a useful resource for the study of further abiotic stress treatments and processes.

StTOC1 binding partners

As TOC1 function has been shown in Arabidopsis to be modified on interaction with other partners (Soy *et al.*, 2016), we aimed to identify the binding partners of potato StTOC1. In yeast two-hybrid screens, TOC1 was found to bind several PRRs and PIF factors, including PIF3 (Soy *et al.*, 2016). This suggests that these interactions may link light signals with TOC1-regulated developmental processes. Interestingly, we demonstrated a conserved interaction of potato StTOC1 and StPIF3, and so the effects on plant height in the potato transgenic lines could be due to StTOC1 inhibition of PIF3 activity (Supplementary Fig. S3). These results also demonstrate that the elongated *StTOC1* antisense phenotype is not associated with decreased tuber yield but reflects the involvement of StTOC1 in additional circadian-regulated processes.

To investigate the role of StTOC1 in *StSP6A* control in more detail, we performed transactivation experiments using the *StSP6A* promoter fused to luciferase. Here, a negative effect of StTOC1 on *StSP6A* expression was observed, which was enhanced when *StSP6A* was co-expressed with *StTOC1* (Fig. 5). This implies that StTOC1 and StSP6A can interact and the resulting complex inhibits *StSP6A* transcription more effectively than StTOC1 on its own. This result is consistent

with the elevated expression levels of *StSP6A* observed on *StTOC1* down-regulation, and shows that the feed-forward loop that leads to amplification of *StSP6A* expression in the stolon can be controlled at elevated temperature by StTOC1.

Previous studies have demonstrated that PIFs play a prominent role in thermomorphogenic hypocotyl elongation in Arabidopsis (Foreman *et al.*, 2011) and that these factors directly bind the *FT* (Arabidopsis *SP6A* ortholog) promoter in a temperature-dependent manner (Kumar *et al.*, 2012). In contrast, potato StPIF3 was unable to activate *StSP6A* expression (Fig. 5), and we presume that PIFs cannot directly bind the *StSP6A* promoter since none of the required E or G-box elements are present within the upstream region of this gene. Additionally, in transactivation experiments, co-infiltration of StPIF3 with StTOC1 effector constructs did not result in more inhibition of *StSP6A* promoter activity than was observed with StTOC1 alone. Inspection of the 2.64 kb promoter fragment used in transactivation assays (Potato Genome Sequencing Consortium, 2011) shows that this region does contain TOC1 recognition motifs (four TGTG sequences 1 kb upstream of the transcription start site). This raises the possibility that StTOC1 directly binds the *StSP6A* promoter, which explains suppression of the *p6A*::LUC reporter on co-infiltration with vectors expressing the StTOC1 protein. An even stronger inhibition of the *StSP6A* promoter (almost 100%) was observed on co-infiltration of StTOC1 and the StSP6A effector constructs. Bimolecular fluorescence complementation and co-immunoprecipitation assays confirmed that StTOC1 does interact with StSP6A, as well as with StPIF3, in addition to dimerizing with itself (Fig. 6). It is also clear that the StTOC1–StPIF3 complex does not inhibit *StSP6A* promoter activity, in contrast to the StTOC1–StSP6A interaction. Thus, these data suggest that StTOC1 inhibits *StSP6A* expression, and hence tuberization, by counteracting the *StSP6A* feed-forward regulatory loop. The elevated expression of *StTOC1* at higher temperature is therefore consistent with the observed reduction in *StSP6A* promoter activity and transcript levels, leading to decreased tuber yields. The enhanced yield of TOCAS lines and reduced tuber yield in StTOC1 overexpressing lines fully supports this regulatory model. In addition, although StTOC1 and StPIF3 can interact, a role for the StTOC1–StPIF3 interaction in the regulation of *StSP6A* promoter activity was not revealed in this study, suggesting that this interaction likely impacts on plant height, as has been observed in Arabidopsis.

Interestingly, recent work has identified a *SP6A*-specific small regulatory RNA that shows enhanced expression under elevated temperatures (Lehretz *et al.*, 2019). The expression of this small RNA provides another mechanism for the temperature regulation of tuberization. These studies illustrate the highly complex tiers of control that have evolved to regulate tuberization, emphasizing the critical nature of this developmental process in the plant life cycle.

Conclusions

Here we extended studies in Arabidopsis linking environmental signals to photomorphogenesis to the crop species potato. We demonstrate that StTOC1 is a temperature-responsive negative regulator of the StSP6A tuberization signal in stolons, and

that StSP6A interacts with StTOC1, resulting in a feedback mechanism that regulates *StSP6A* expression. These studies add to our current understanding of tuberization control and demonstrate a main integration mechanism of thermal and developmental signalling via a circadian clock core component.

Supplementary data

Supplementary data are available at *JXB* online.

Fig. S1. Comparison of plant height of glasshouse-grown Desiree *StTOC1* transgenic lines with WT plants.

Fig. S2. Whole-plant tuber yield from WT and TOCAS44 grown at normal and elevated temperatures.

Fig. S3. Protein–protein interactions between StTOC1, StPIF3, and StSP6A.

Fig. S4. Localization of GFP-tagged proteins for StPIF3, StTOC1, and SP6A following infiltration of *Nicotiana benthamiana* leaves.

Fig. S5. Comparison of gene co-expression profiles by *K*-means clustering into four gene sets.

Table S1. Gene expression data from swelling stolons in Desiree WT and TOCAS44 associated with starch metabolism, starch degradation, transcription factors related to starch metabolism, and heat shock genes.

Table S2. Lists of genes represented in *K*-means clusters described in Supplementary Fig. S5.

Table S3. Primer/probe sequences used in this study.

Acknowledgements

References

Abelenda JA, Cruz-Oró E, Franco-Zorrilla JM, Prat S. 2016. Potato StCONSTANS-like1 suppresses storage organ formation by directly activating the FT-like *StSP5G* repressor. Current Biology **26**, 872–881.

Abelenda JA, Navarro C, Prat S. 2011. From the model to the crop: genes controlling tuber formation in potato. Current Opinion in Biotechnology **22**, 287–292.

Belda-Palazón B, Ruiz L, Marti E, Tarraga S, Tiburcio AF, Culianez F, Farras R, Carrasco P, Ferrando A. 2012. Aminopropyltransferases involved in polyamine biosynthesis localize preferentially in the nucleus of plant cells. PLoS One **7**, e46907.

Birch PR, Bryan G, Fenton B, Gilroy EM, Hein I, Jones JT, Prashar A, Taylor MA, Torrance L, Toth IK. 2012. Crops that feed the world 8: potato: are the trends of increased global production sustainable? Food Security **4**, 477–508.

Bos JI, Armstrong MR, Gilroy EM, et al. 2010. *Phytophthora infestans* effector AVR3a is essential for virulence and manipulates host plant immunity by stabilizing host E3 ligase CMPG1. Proceedings of the National Academy of Sciences, USA **107**, 9909–9914.

Campbell R, Ducreux LJ, Morris WL, Morris JA, Suttle JC, Ramsay G, Bryan GJ, Hedley PE, Taylor MA. 2010. The metabolic and developmental roles of carotenoid cleavage dioxygenase4 from potato. Plant Physiology **154**, 656–664.

Ducreux LJ, Morris WL, Prosser IM, Morris JA, Beale MH, Wright F, Shepherd T, Bryan GJ, Hedley PE, Taylor MA. 2008. Expression profiling of potato germplasm differentiated in quality traits leads to the identification of candidate flavour and texture genes. Journal of Experimental Botany **59**, 4219–4231.

Eriksson ME, Webb AA. 2011. Plant cell responses to cold are all about timing. Current Opinion in Plant Biology **14**, 731–737.

Ewing EE. 1978. Shoot, stolon, and tuber formation on potato (*Solanum tuberosum* L.) cuttings in response to photoperiod. Plant Physiology **61**, 348–353.

Ewing EE. 1981. Heat stress and the tuberization stimulus. American Potato Journal **58**, 31–49.

Ferreira, SJ, Senning M, Sonnewald S, Keßling PM, Goldstein R, Sonnewald U. 2010. Comparative transcriptome analysis coupled to X-ray CT reveals sucrose supply and growth velocity as major determinants of potato tuber starch biosynthesis. BMC Genomics **11**, 93.

Foreman J, Johansson H, Hornitschek P, Josse EM, Fankhauser C, Halliday KJ. 2011. Light receptor action is critical for maintaining plant biomass at warm ambient temperatures. The Plant Journal **65**, 441–452.

Gendron JM, Pruneda-Paz JL, Doherty CJ, Gross AM, Kang SE, Kay SA. 2012. *Arabidopsis* circadian clock protein, TOC1, is a DNA-binding transcription factor. Proceedings of the National Academy of Sciences, USA **109**, 3167–3172.

George TS, Taylor MA, Dodd IC, White PJ. 2018. Climate change and consequences for potato production: a review of tolerance to emerging abiotic stress. Potato Research 1–30.

Guerineau F, Brooks L, Meadows J, Lucy A, Robinson C, Mullineaux P. 1990. Sulfonamide resistance gene for plant transformation. Plant Molecular Biology **15**, 127–136.

Halford NG, Foyer CH. 2015. Producing a road map that enables plants to cope with future climate change. Journal of Experimental Botany **66**, 3433–3434.

Han Y, Chen Y, Yin S, Zhang M, Wang W. 2015. Over-expression of *TaEXPB23*, a wheat expansin gene, improves oxidative stress tolerance in transgenic tobacco plants. Journal of Plant Physiology **173**, 62–71.

Hancock RD, Morris WL, Ducreux LJ, et al. 2014. Physiological, biochemical and molecular responses of the potato (*Solanum tuberosum* L.) plant to moderately elevated temperature. Plant, Cell & Environment **37**, 439–450.

Huang W, Pérez-García P, Pokhilko A, Millar AJ, Antoshechkin I, Riechmann JL, Mas P. 2012. Mapping the core of the *Arabidopsis* circadian clock defines the network structure of the oscillator. Science **336**, 75–79.

Kloosterman B, Abelenda JA, Carretero Gomez M del M, et al. 2013. Naturally occurring allele diversity allows potato cultivation in northern latitudes. Nature **495**, 246–250.

Kumar SV, Lucyshyn D, Jaeger KE, Alós E, Alvey E, Harberd NP, Wigge PA. 2012. Transcription factor PIF4 controls the thermosensory activation of flowering. Nature **484**, 242–245.

Legnaioli T, Cuevas J, Mas P. 2009. TOC1 functions as a molecular switch connecting the circadian clock with plant responses to drought. The EMBO Journal **28**, 3745–3757.

Lehretz GG, Sonnewald S, Hornyik C, Corral JM, Sonnewald U. 2019. Post-transcriptional regulation of *FLOWERING LOCUS T* modulates heat-dependent source-sink development in potato. Current Biology **29**, 1614–1624.e3.

Levy D, Veilleux RE. 2007. Adaptation of potato to high temperatures and salinity—a review. American Journal of Potato Research **84**, 487–506.

Más P, Alabadí D, Yanovsky MJ, Oyama T, Kay SA. 2003. Dual role of TOC1 in the control of circadian and photomorphogenic responses in Arabidopsis. The Plant Cell **15**, 223–236.

Más P, Kim WY, Somers DE, Kay SA. 2003. Targeted degradation of TOC1 by ZTL modulates circadian function in *Arabidopsis thaliana*. Nature **426**, 567–570.

Matsushika A, Makino S, Kojima M, Mizuno T. 2000. Circadian waves of expression of the APRR1/TOC1 family of pseudo-response regulators in *Arabidopsis thaliana*: insight into the plant circadian clock. Plant & Cell Physiology **41**, 1002–1012.

Morris WL, Hancock RD, Ducreux LJ, *et al*. 2014. Day length dependent restructuring of the leaf transcriptome and metabolome in potato genotypes with contrasting tuberization phenotypes. Plant, Cell & Environment **37**, 1351–1363.

Murashige T, Skoog F. 1962. A revised medium for rapid growth and bio assays with tobacco tissue cultures. Physiologia Plantarum **15**, 473–497.

Nagarajan S, Minhas JS. 1995. Internodal elongation: a potential screening technique for heat tolerance in potato. Potato Research **38**, 179–186.

Nakamichi N, Kiba T, Kamioka M, Suzuki T, Yamashino T, Higashiyama T, Sakakibara H, Mizuno T. 2012. Transcriptional repressor PRR5 directly regulates clock-output pathways. Proceedings of the National Academy of Sciences, USA **109**, 17123–17128.

Navarro C, Abelenda JA, Cruz-Oró E, Cuéllar CA, Tamaki S, Silva J, Shimamoto K, Prat S. 2011. Control of flowering and storage organ formation in potato by FLOWERING LOCUS T. Nature **478**, 119–122.

Nicot N, Hausman JF, Hoffmann L, Evers D. 2005. Housekeeping gene selection for real-time RT-PCR normalization in potato during biotic and abiotic stress. Journal of Experimental Botany **56**, 2907–2914.

Pokhilko A, Mas P, Millar AJ. 2013. Modelling the widespread effects of TOC1 signalling on the plant circadian clock and its outputs. BMC Systems Biology **7**, 23.

Possart A, Xu T, Paik I, *et al*. 2017. Characterization of phytochrome interacting factors from the moss *Physcomitrella patens* illustrates conservation of phytochrome signaling modules in land plants. The Plant Cell **29**, 310–330.

Reynolds MP, Ewing EE, Owens TG. 1990. Photosynthesis at high temperature in tuber-bearing *Solanum* species: a comparison between accessions of contrasting heat tolerance. Plant Physiology **93**, 791–797.

Schmittgen TD, Livak KJ. 2008. Analyzing real-time PCR data by the comparative C_T method. Nature Protocols **3**, 1101–1108.

Soy J, Leivar P, González-Schain N, Martín G, Diaz C, Sentandreu M, Al-Sady B, Quail PH, Monte E. 2016. Molecular convergence of clock and photosensory pathways through STPIF3–TOC1 interaction and co-occupancy of target promoters. Proceedings of the National Academy of Sciences, USA **113**, 4870–4875.

Strayer C, Oyama T, Schultz TF, Raman R, Somers DE, Más P, Panda S, Kreps JA, Kay SA. 2000. Cloning of the *Arabidopsis* clock gene *TOC1*, an autoregulatory response regulator homolog. Science **289**, 768–771.

The Potato Genome Sequencing Consortium. 2011. Genome sequence and analysis of the tuber crop potato. Nature **475**, 189–195.

Tian T, Liu Y, Yan H, You Q, Yi X, Du Z, Xu W, Su Z. 2017. agriGO v2.0: a GO analysis toolkit for the agricultural community, 2017 update. Nucleic Acids Research **45**, W122–W129.

Trapero-Mozos, A, Morris WL, Ducreux LJ, McLean K, Stephens J, Torrance L, Bryan GJ, Hancock RD, Taylor MA. 2018. Engineering heat tolerance in potato by temperature-dependent expression of a specific allele of *HEAT-SHOCK COGNATE 70*. Plant Biotechnology Journal **16**, 197–207.

Van Harsselaar JK, Lorenz J, Senning M, Sonnewald U, Sonnewald S. 2017. Genome-wide analysis of starch metabolism genes in potato (*Solanum tuberosum* L.). BMC Genomics **18**, 37.

Wang W, Barnaby JY, Tada Y, Li H, Tör M, Caldelari D, Lee DU, Fu XD, Dong X. 2011. Timing of plant immune responses by a central circadian regulator. Nature **470**, 110–114.

Wenkel S, Turck F, Singer K, Gissot L, Le Gourrierec J, Samach A, Coupland G. 2006. CONSTANS and the CCAAT box binding complex share a functionally important domain and interact to regulate flowering of *Arabidopsis*. The Plant Cell **18**, 2971–2984.

Wolf S, Marani A, Rudich J. 1991. Effect of temperature on carbohydrate metabolism in potato plants. Journal of Experimental Botany **42**, 619–625.

Zhan Z, Zhang C, Zhang H, Li X, Wen C, Liang Y. 2017. Molecular cloning, expression analysis, and subcellular localization of *FLOWERING LOCUS T* (*FT*) in carrot (*Daucus carota* L.). Molecular Breeding **37**, 149.